The Hydraulic Buck Converter Exploiting the Load Capacitance

DI Helmut Kogler

Institute of Machine Design and Hydraulic Drives, Johannes Kepler University Linz, Altenbergerstrasse 69, 4040 Linz, E-mail: helmut.kogler@jku.at

Professor Dr. Rudolf Scheidl

Institute of Machine Design and Hydraulic Drives, Johannes Kepler University Linz, Altenbergerstrasse 69, 4040 Linz, E-mail: rudolf.scheidl@jku.at

Abstract

The hydraulic buck converter requires a pressure attenuation device at its output to smoothen the pressure ripples excited by the switching process. For this purpose often gas filled accumulators are used. Such accumulators' installation with low hydraulic impedance is challenging and maintenance causes and extra effort. Furthermore, the nonlinear behavior of the gas spring is often unwanted. A number of applications, especially high force hydraulics, use huge cylinders with a correspondingly high fluid volume which may have sufficient capacitance for pressure attenuation. Additionally, a phase shifted operation of several parallel hydraulic buck converters reduces the pressure pulsations by increasing the effective switching frequency at the load. This paper investigates such a multi hydraulic buck converter arrangement with a phase shifted operation and with just the cylinder capacitance for pressure attenuation.

KEYWORDS: digital hydraulics, switching converter, buck converter

1. Introduction

The idea to exploit switching control, which is common in modern electrical machines, also in hydraulics has the first time been tested by an American research group in 1988 /1/. Switching control means to use on-off valves which are periodically switched, e.g. in PWM mode, to control the system. From the mid nineties of the last century on, different other groups published ideas and research results concerning hydraulic switching control /2/ to /6/.

The hydraulic buck converter (HBC) corresponds directly to its electrical pendant. This standard circuitry of modern electric power supply units generates the required low voltage DC supply from the electric net. Both buck converter circuitries, the electrical and the hydraulic, are shown in **Figure 1**.
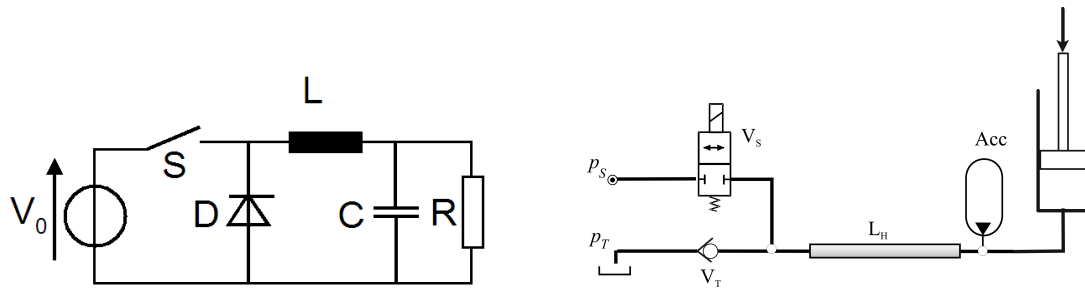
Figure 1: The electrical and the hydraulic buck converter; equivalent components: S~V_S, D~V_T, L~L_H, C~Acc; remark: for the sake of direct comparison the hydraulic converter is shown only with one active valve V_S; to lower the load a second active valve connecting the system with the tank line is required.

/6, 7, 8/ present results of the authors' research on the buck converter, run in a PWM mode of operation, concerning efficiency and dynamical performance. They show theoretically and experimentally that a decisive gain in efficiency can be obtained. In particular, energy can be also recuperated, if a second active on-off valve is provided, as mentioned in the caption of Figure 1.

Major challenges of the HBC are its components. Fast switching valves are required with a durable switching frequency in the range of > 50 Hz to render a compact design of the hydraulic inductance (L_H) and of the accumulator (Acc) possible. The inductance, which is just a straight or curved pipe, is suffering from the trade-off between high-inductance, low resistance, and low capacitance. Shrinking the pipe diameter increases the inductance and shrinks the capacitance – which is wanted – but same time increases resistance which deteriorates efficiency. The accumulator has to flatten pressure ripples and is exposed to high frequency impulsive load. Standard accumulator technologies can hardly compete with these requirements and extra measures have to be taken to provide the required performance.

Accumulators based on a gas spring only work above their charge pressure and exhibit a fairly nonlinear behavior. Furthermore, large capacitance makes the system soft. Though the latter can be compensated by advanced control techniques (see, e.g. /9/), it is desirable to keep the accumulator small or to avoid it at all. Avoidance of capacitors or at least capacitance reduction is also a point of interest in power electronics, since capacitors are the components limiting the lifetime, in particular if electrolytic capacitors have to be used. In /10/ a power electronic circuitry and a corresponding switching strategy are presented by means of which capacitors can be avoided.

In this paper the avoidance of the load sided hydraulic accumulators (Acc in Figure 1) is discussed. Avoidance is based on two features: i) the exploitation of the hydraulic capacitance of the cylinder and ii) the application of two or more buck converters which are run in a phase shifted mode. It is a theoretical study using analytical and numerical methods which have been verified by several buck converter experiments in the past.

2. Multiple hydraulic buck converters actuating one load

Figure 2 shows the hydraulic system under study. A double acting cylinder acting against a process force F_P is connected to system pressure p_S at its rod side and to the multiple (number N) HBCs at its piston side. For the further it is assumed that the acting of the individual HBCs, i.e. the switching of their pressure and tank sided valves ($V_{S,n}$, $V_{T,n}$), is phase shifted by a phase angle $2\pi/N$. If the switching frequency is f_{SW} the time delay of switching the n-th valve ($V_{S,n}$ or $V_{T,n}$, respectively) relative to the first valve ($V_{S,1}$ or $V_{T,1}$, respectively) is
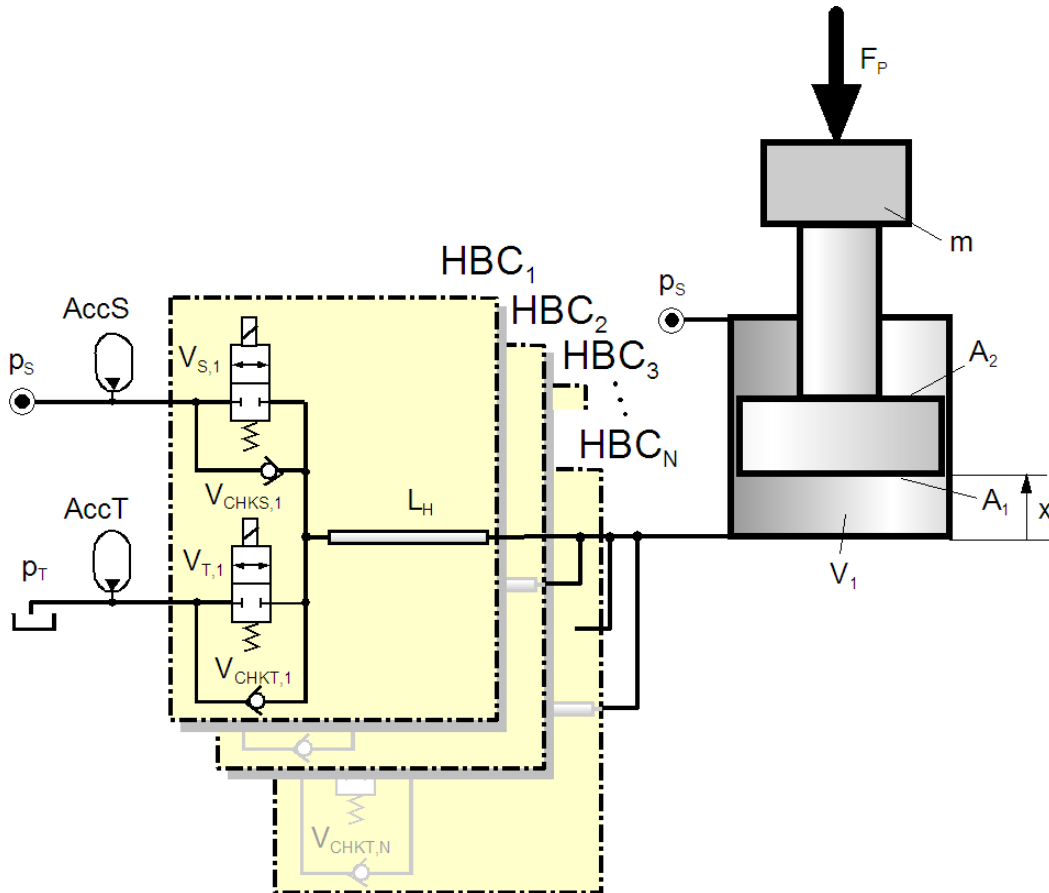
$$\Delta t_n = \frac{(n-1)}{f_{SW} N}.$$

(1)

Figure 2: A hydraulic linear drive controlled by N hydraulic buck converters.

2.1. Simplified, nondimensional mathematical model

The simplified, nondimensional mathematical model which provides the basis for an assessment of the pros and cons of N HBCs instead of only one is a combination of the previous models presented in /6/ and /11/.
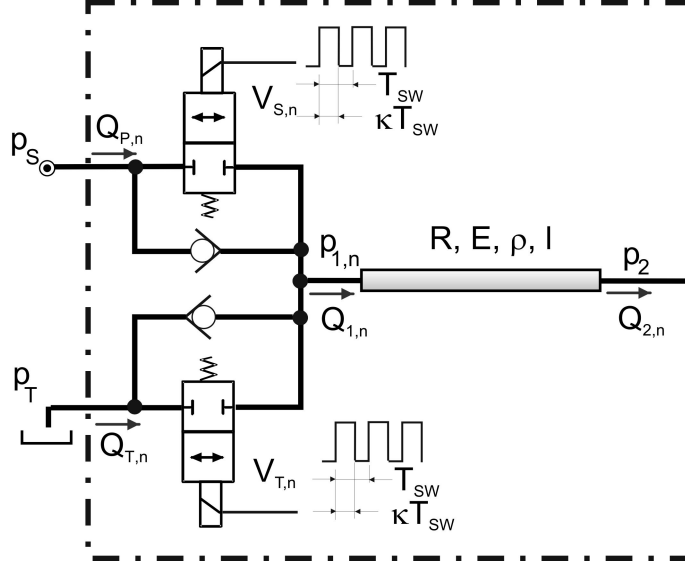

Figure 3: Schematic and nomenclature of the HBC model.

It employs the following scales for nondimensionalization (they refer also to the states of the cylinder; see Figure 2).

$$Q_{i,n} = \frac{1}{\omega_0}\frac{p_S R^2 \pi}{\rho l} q_{i,n}; \; p_{1,n} = \psi_{1,n} p_S; \; p_2 = \psi_2 p_S; \; p_T = \psi_T p_S; \; x = \xi X; \; t = \omega_0 \tau$$

$$r' = R\sqrt{\frac{c}{l\nu}}; \; a = \frac{X A_1}{V_0}; \; \varepsilon = \frac{p_S}{E}; \; b = \frac{p_S R^2 \pi}{\omega_0^2 \rho l V_0}; \quad \omega_0 = \frac{c}{l}; \; c = \sqrt{\frac{E}{\rho}}; \; j = +\sqrt{-1}$$

(2)

$Q_{i,n}$ and $q_{i,n}$ are the physical and nondimensional pairs of the flow rates (i = S, T, 1, 2) of the n-th HBC, p_k and ψ_k the pressure pairs (k = S, T, 1, 2), t, τ the time pairs, ω, Ω the angular frequency pair, ω_0 the scaling frequency, R, r' the inductance pipe radius pair, l the pipe length, X is the maximum stroke of the piston, A_1 the piston area, V_0 the hydraulic dead volume for the retracted piston, ν the kinematic fluid viscosity, c the wave propagation speed, E the fluid bulk modulus, and ρ the fluid density. The nondimensional state equations of that system consider the dynamics of the inductance pipe by frequency domain model (3) according to /11/.

$$\hat{q}_{1,n} = -j \frac{\hat{\psi}_{1,n} \cos\left(\sqrt{\Omega}\left(\sqrt{\Omega} + \frac{1-j}{r'\sqrt{2}}\right)\right) - \hat{\psi}_2}{\left(1 + \frac{1-j}{r'\sqrt{\Omega}\sqrt{2}}\right)\sin\left(\sqrt{\Omega}\left(\sqrt{\Omega} + \frac{1-j}{r'\sqrt{2}}\right)\right)}$$

$$\hat{q}_{2,n} = -j \frac{\left(\hat{\psi}_{1,n} - \hat{\psi}_2 \cos\left(\sqrt{\Omega}\left(\sqrt{\Omega} + \frac{1-j}{r'\sqrt{2}}\right)\right)\right)}{\left(1 + \frac{1-j}{r'\sqrt{\Omega}\sqrt{2}}\right)\sin\left(\sqrt{\Omega}\left(\sqrt{\Omega} + \frac{1-j}{r'\sqrt{2}}\right)\right)}$$

(3)

The hat (^) indicates the Fourier transform of a variable according to (4)

$$\hat{q}_{i,n}(\Omega) = \int_{-\infty}^{\infty} q_{i,n}(\tau)e^{j\Omega\tau}d\tau, i = 1,2$$

$$\hat{\psi}_{i,n}(\Omega) = \int_{-\infty}^{\infty} \psi_{i,n}(\tau)e^{j\Omega\tau}d\tau, i = 1,2,$$

(4)

The pressure buildup equation in the piston chamber and its frequency domain approximation (change of piston position x is neglected) and the momentum equation of the piston are given in (5) and (6), respectively.

$$\dot{p}_2 = \frac{E}{V_0 + xA_1}\left(\sum_{n=1}^{N} Q_{2,n} - \dot{x}A_1\right)$$

$$\varepsilon\Omega\hat{\psi}_2 = \frac{1}{1+a\xi}\left(b\sum_{n=1}^{N}\hat{q}_{2,n} - a\Omega\hat{\xi}\right)$$

(5)

$$m\ddot{x} = p_2 A_1 - p_S A_2 - F_P$$

$$\hat{\xi} = \frac{1}{\Omega^2}\frac{p_S A_1}{\omega_0^2 Xm}\left(\hat{\psi}_2 - \frac{A_2}{A_1} - \frac{F_P}{p_S A_1}\right)$$

(6)

In order to estimate the effect of using N smaller HBCs instead of one larger HBC by a quite simple model, the following simplifying assumptions are made. The effect of the piston motion on the pressure pulsation (role of $\hat{\xi}$ in Eq. (5)) is negligible. The pulsation is studied for the retracted piston ($\xi = 0$), which is the worst case. If (5) is evaluated, the following formula results

$$\hat{\psi}_2 = \frac{1}{\Omega}\frac{R^2\pi l}{V_0}\sum_{n=1}^{N}\hat{q}_{2,n} = \frac{1}{\Omega}\frac{V_{Pipe}}{V_0}\sum_{n=1}^{N}\hat{q}_{2,n},$$

(7)

According to (7) the pressure pulsation is the sum of all flow rate pulsations times the ratio of the inductance pipe volume V_{Pipe} and the dead volume V_0 of the cylinder chamber.

In a steady state operation an essentially periodic behavior can be expected resulting in a discrete spectrum of all states. This is of course not fully true for ξ, but if its change rate is small compared to the switching frequency Ω_{SW}, this assumption is justified.

The flow rate $q_{2,n}(\tau)$ contributed by the n-th pipe can be represented by a Fourier series with the fundamental frequency Ω_{SW} as given by (8) since the n-th HBC operates with a phase shift of $2\pi\,(n\text{-}1)/N$.

$$q_{2,n}(\tau) = \sum_{k=0}^{\infty} \hat{q}_{2,n,k}\, e^{jk\Omega_{SW}\tau} = \sum_{k=0}^{\infty} \hat{q}_{2,1,k}\; e^{jk\left(\Omega_{SW}\tau + \frac{2\pi(n-1)}{N}\right)} \tag{8}$$

By inserting (8) in (7), the pressure fluctuation in the cylinder of n HBCs can be written as follows

$$\psi_2(\tau) = \frac{V_{Pipe}}{V_0} \sum_{k=1}^{\infty} \left[\hat{q}_{2,1,k} \sum_{n=1}^{N} e^{jk\left(\Omega_{SW}\tau + \frac{2\pi(n-1)}{N}\right)} \right] =$$
$$\frac{V_{Pipe}}{V_0} \sum_{k=1}^{\infty} \left[\hat{q}_{2,1,k}\, e^{jk\Omega_{SW}\tau} \sum_{n=1}^{N} e^{jk\frac{2\pi(n-1)}{N}} \right] \tag{9}$$

The pulsation attenuation effect of N converters operating in a phase shifted mode is represented by the last sum in (9). Its absolute value is

$$\sum_{n=1}^{N} e^{jk\frac{2\pi(n-1)}{N}} = \begin{cases} N & \text{if} \quad k = \gamma N \\ 0 & \text{else} \end{cases} \quad ; \gamma \text{ is any positive integer number.} \tag{10}$$

Thus, only frequencies of order $k = \gamma N$ are present and their pulsation amplitude generated by all N converters is N times that of one pipe, all other frequencies are cancelled. Considering that each of the N converters delivers only 1/N-th that of one converter in case N = 1, this N times pulsation amplitude indicated by the result of (10) is no change for the worse. Quite the contrary, there is a strong reduction in pulsation by employing N converters resulting from two effects:

1. The order N amplitude is typically much smaller than the order 1 amplitude. They decrease at least by a factor 1/N if ψ_1 is a rectangular signal and with

even higher order in N for a ramp type ψ_1 - signal which is the case because of the finite response dynamics of the switching valve.

2. The hydraulic capacitance filters flow pulsation due to its integrating nature by $1/\Omega = 1/(N^*\Omega_{SW})$ (see Eq. (7)).

Thus, the improvement in pulsation reduction at the load rises quadratically with N.

3. Numerical simulations

A configuration according to Figure 2 is modeled. It represents a high force application. The cylinder areas are $A_1 \approx 1.2 m^2$, $A_2 \approx 0.6 m^2$ and the dead volume in the piston chamber is $V_0 \approx 150 l$, which is sufficient for a good pressure attenuation in case of a phase shifted HBC configuration. A typical velocity for positioning the piston is 4 mm/s, which requires a flow rate of about 300 l/min in this case. Such large flow rates cannot be reasonably handled by a single hydraulic buck converter with state of the art switching valves. Thus, the following simulations consider 6 HBCs in parallel, which operate at a switching frequency of 50 Hz. The pipe inductance of one individual HBC is about 2.5 m with a hydraulic diameter of 10 mm. Also the effect of wave propagation in the fluid is accounted for by a linear method of characteristics in the simulation model. The switching valves of the converter have a nominal size of 40 l/min and the check valves of 120 l/min, each at a nominal pressure drop of 5 bar. The dynamics of the digital valves is represented by a ramp with a rise time of 1 ms.

In the simulations three different configurations are compared. The reference case is a conventional servo drive in plunger mode. The servo valve has a nominal flow rate of 400 l/min at a nominal pressure drop of 35 bar and acts as a $3/3$-valve. The servo valve dynamics is taken into account by a PT-2 element with a cut-off frequency of 100 Hz. The mentioned reference servo drive is compared to two different HBC clusters, each consisting of 6 parallel converters. The first HBC cluster is pulsed synchronously, i.e., each switching valves of each converter are switched at the same time for the same duty ratio. On the other hand the individual HBCs of the second multi HBC configuration are controlled with a phase shift according to Eq. (1) with $N = 6$ and $f_{SW} = 50Hz$. In this case, the PWM duty cycle of each converter is equal for one switching period.

In the following, two different operating scenarios are investigated. First, a positioning of the piston in form of a ramp with constant slope and, second, the reaction to a

trapezoidal load force variation are studied. Both cases are closed loop controlled by a simple P-controller. All simulations were carried out in Matlab/Simulink.

3.1. Movement of the Piston

Figure 4 depicts the simulation results for the positioning motion with 4 *mm/s* ramp speed. In the left diagrams the synchronous HBCs operation and on the right diagrams the phase shifted HBCs operation are compared to the hydraulic proportional servo drive (HPD). The diagrams show top-down the positions, the velocities, and the energy consumptions of the different configurations.
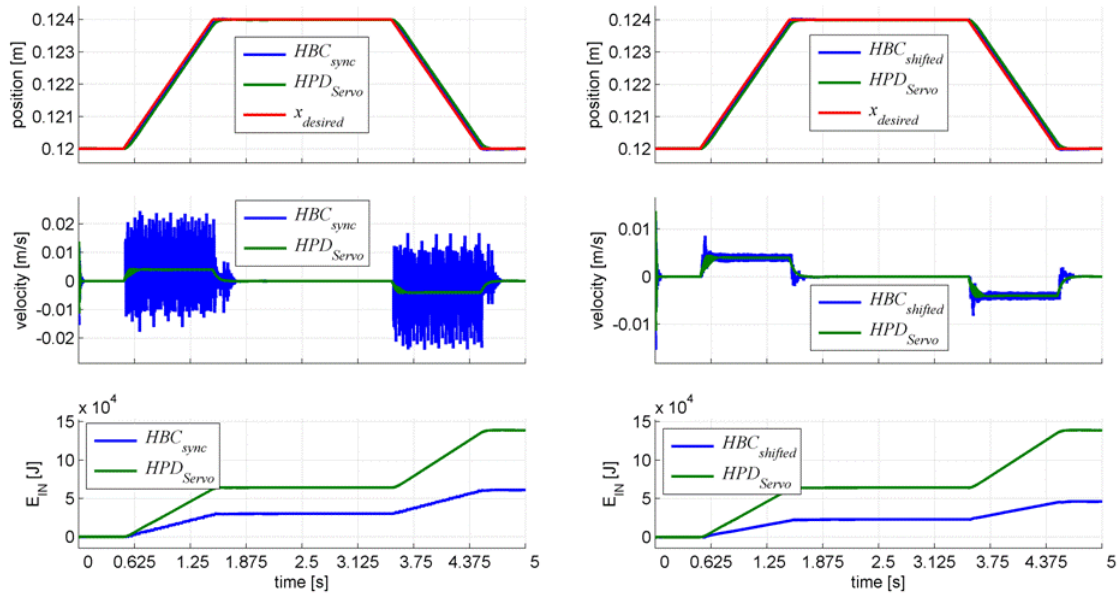

Figure 4: Simulation results of a linear hydraulic drive for a position ramp with a slope of 4 *mm/s* controlled by N HBCs compared to a conventional servo drive (HPD); left: synchronized operation of HBCs; right: phase shifted operation of HBCs.

The piston velocity of the synchronously pulsed converters fluctuates quite strongly, because the flow rate pulses of all HBCs arrive at the cylinder coincidently. Furthermore, the natural frequency of the mass loaded cylinder is higher than the switching frequency of the converter cluster. Consequently, the piston follows the flow pulsation quite directly since the inertial impedance is low. The phase shifted configuration shows dramatically lower velocity fluctuations than the synchronously switched drive. The noticed switching frequency in the cylinder is 300 *Hz* due to the phase shifted control of the individual HBCs, which is sufficiently above the natural frequency of the load system to prevent unwanted ripples in the movement. In the lower diagrams the remarkable energy saving of the hydraulic buck converter becomes

clear. For the complete working cycle the HBC configurations need less than half of the energy of a servo drive.

3.2. Performance due to a certain load force

In **Figure 5 and Figure 6** the simulated systems' responses to a process force variation of $15\ MN$ are shown. Figure 5 illustrates the synchronous mode. On the figure's left hand side the piston position, the piston velocity of the HBC cluster and of the servo drive are depicted. On the right hand side the corresponding pressure signals, the load force and the consumed energy are presented. The maximum deviations from the desired position are in the range of 200 microns for both drive systems. The HBC position oscillates with a high frequency but is able to recuperate about half of the compression energy, built up by the rising process force, when the force is released.
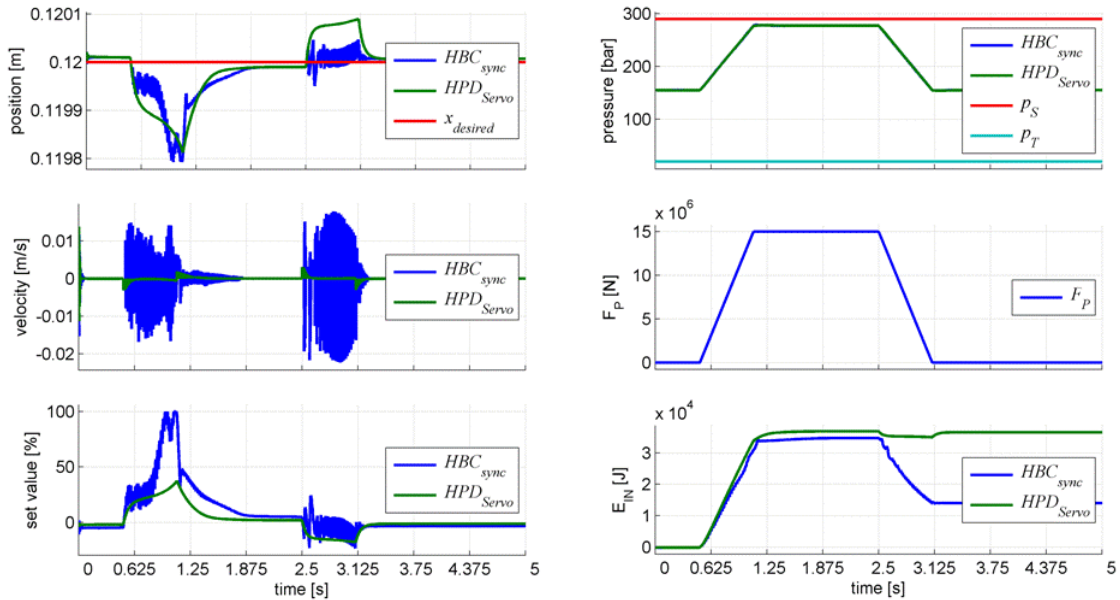

Figure 5: Performance of the synchronized configuration at a process force of $15\ MN$ compared to a conventional servo drive (HPD).

In Figure 6 the simulation results of the phase shifted approach are illustrated, which shows an equivalent performance as the conventional servo drive in terms of positioning accuracy but at half of its energy consumption. The phase shifted operation of the HBCs creates low flow rate pulses at high frequencies. Therefore, a smoother flow rate is achieved than with the synchronously switching HBCs. In turn, less pressure fluctuations are excited in the cylinder chamber, which results in higher accuracy. Due to the high dynamics, i.e. the short switching times, of the digital valves

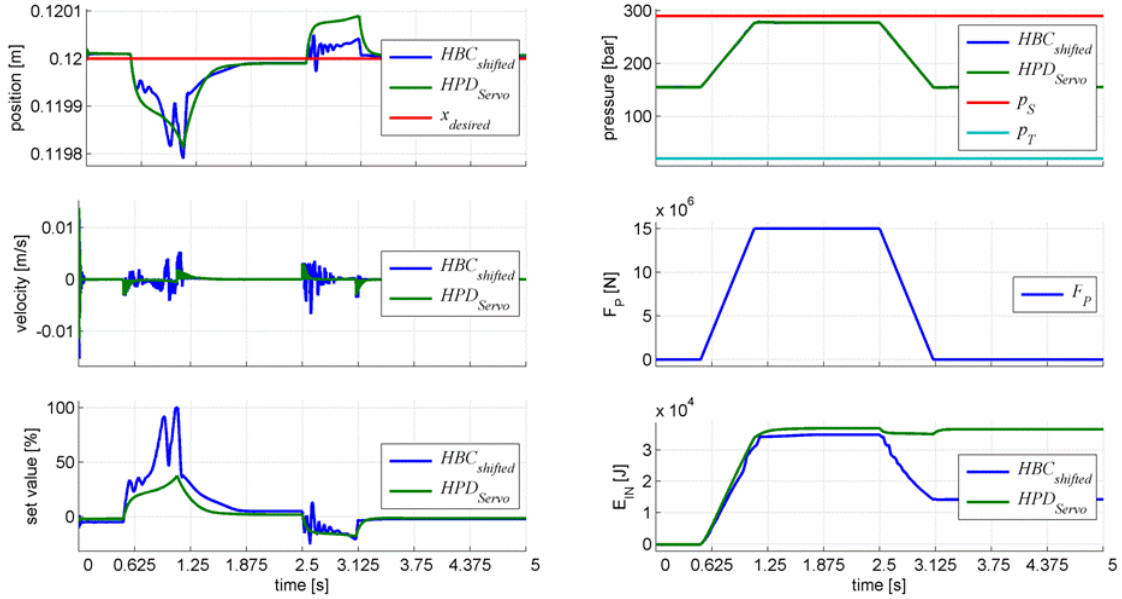of the HBCs, the switching configuration achieves even a faster response to load fluctuations than the HPD.

Figure 6: Performance of the phase shifted configuration at a process force of $15\ MN$ compared to a conventional servo drive (HPD).

4. Conclusions

In this paper the application of a hydraulic drive controlled by a multi HBC configuration exploiting the load capacity was discussed. It was clearly shown, that a phase shifted operation of several hydraulic buck converters reduces the pressure pulsations due to switching at the load significantly. The simulation results taught that with the phase shifted HBC operation the accuracy in load positioning is comparable with a common proportional servo drive, even at high load forces. Moreover, due to the high bandwidth of the switching valves the HBC control achieves even a better dynamic response. Furthermore, the energy consumption of the considered linear hydraulic drive can be reduced dramatically by the HBC. This may not only lower energy costs, but also the installation costs, since a smaller hydraulic power supply unit is required.

5. Acknowledgement

6. References

/1/   F. T. Brown, S. C. Tentarelli and S. Ramachandran A hydraulic rotary switched-inertance servo-transformer. ASME J. Dynamic Systems, Meas. and Cont., Vol. 110, No. 2, pp. 144-150, 1988.

/2/   H. Gall, K. Senn. Freilaufventile - Ansteuerungskonzept zur Energieeinsparung bei hydraulischen Linearantrieben. O+P "Ölhydraulik und Pneumatik" 38, Nr.1-2, 1994.

/3/   R. Scheidl, D. Schindler, G. Riha, and W. Leitner, Basics for the Energy-Efficient Control of Hydraulic Drives by Switching Techniques, Proceedings of the 3rd Conference on Mechatronics and Robotics, in J. Lückel, Teubner, 1995.

/4/   R. Scheidl, M. Garstenauer, and S. Grammer, The Resonance Converter – A Novel Method for Hydraulic Fluid Power Control, Proceedings of Mechatronics '96, Guimaraes, Portugal, 9-1996.

/5/   J. Dantlgraber. Hydro-Transformer. European patent application (PCT) Intern. Publication No. WO 00/08339, 2000.

/6/   R. Scheidl, B. Manhartsgruber, H. Kogler, B. Winkler, M. Mairhofer. The Hydraulic Buck Converter - Concept and Experimental Results, Proc. 6th IFK, 6. International Fluid Power Conference, Dresden, 31.3.-2.4. 2008.

/7/   E. Guglielmino, C. Semini, Y. Yang, D. Caldwell, R. Scheidl, H. Kogler. Energy Efficient Fluid power in Autonomous Legged Robots, Proc. 2009 ASME Dynamic Systems and Control Conference, Renaissance Hollywood Hotel, October 12-14, 2009, Hollywood, California.

/8/   H. Kogler, R. Scheidl, M. Ehrentraut, E. Guglielmino, C. Semini, D. Caldwell. A Compact Hydraulic Switching Converter for Robotic Applications. Proc. Bath/ ASME Symposium on Fluid Power and Motion Control - FPMC2010,, Sept. 15-17 2010, Bath, UK, pp. 56-68.

/9/   H. Kogler, R. Scheidl. Hydraulic Switching Control of Resonant Drives. Proc. Mechatronics 2010 (Book 2/2), June 28-30, 2010, Zurich, Switzerland, pp. 97-102.

/10/   M. Huber, Reduction and Elimination of Electrolytic Capacitors in Power Electronics of Automotive Applications, PhD-Thesis, Institute of Electrical Drives and Power Electronics, Johannes Kepler University, Linz, 2006.

/11/   R. Scheidl, B. Manhartsgruber, and H. Kogler. Mixed time–frequency domain simulation of a hydraulic inductance pipe with a check valve. Proceedings of the Institution of Mechanical Engineers, Part C: Journal of Mechanical Engineering Science, October 2011; vol. 225, 10: pp. 2413-2421.

6.1. Nomenclature

a	nondimensional cross-section	1
A_1	piston sided cross-section	m^2
A_2	annulus cross-section	m^2
b	scaling parameter	1
c	wave speed	m/s
Δt_n	time delay of nth switching valve	s
E	bulk modulus of oil	Pa
ε	nondimensional capacity	1
f_{SW}	switching frequency	$1/s$
j	imaginary unit	$\sqrt{-1}$
k	counter variable	1
l	pipe length	m
m	mass of dead load	kg
n	index of nth converter	1
N	number of converters	1
p_1	pressure in the piston sided chamber	Pa
p_2	pressure in the annulus chamber	Pa
p_S	supply pressure	Pa
p_T	tank pressure	Pa

$\psi_{i,n}$	nondimensional pressure at i^{th} pipe end of the nth HBC in time domain	1
$\hat{\psi}_{i,n}$	nondimensional pressure at i^{th} pipe end of the nth HBC in frequency domain	1
$Q_{i,n}$	physical flow rate at i^{th} pipe end of the nth HBC in time domain	m^3/s
$q_{i,n}$	nondimensional flow rate at i^{th} pipe end of the nth HBC in time domain	1
$\hat{q}_{i,n}$	nondimensional flow rate at i^{th} pipe end of the nth HBC in time domain	1
r'	nondimensional radius of the pipe	1
R	pipe radius	m
ρ	fluid density	kg/m^3
t	time	s
τ	nondimensional time	1
V_0	dead volume of the cylinder	m^3
V_{Pipe}	volume of inductance pipe	m^3
v	piston velocity	m/s
x	piston position	m
X	effective length of cylinder	m
ξ	nondimensional piston position in time domain	1
$\hat{\xi}$	nondimensional piston position in frequency domain	1
ω_0	characteristic angular frequency	rad/s
Ω	nondimensional angular frequency	1
Ω_{SW}	nondimensional switching frequency	1